Protein−Sulfenic Acids: Diverse Roles for an Unlikely Player in Enzyme Catalysis and Redox Regulation †

ARTICLE *in* BIOCHEMISTRY · DECEMBER 1999

Impact Factor: 3.02 · DOI: 10.1021/bi992025k · Source: PubMed

7 AUTHORS, INCLUDING:

Derek Parsonage
Wake Forest School of Medicine
92 PUBLICATIONS **2,470** CITATIONS

SEE PROFILE

Biochemistry

 Volume 38, Number 47 November 23, 1999

Perspectives in Biochemistry

Protein-Sulfenic Acids: Diverse Roles for an Unlikely Player in Enzyme Catalysis and Redox Regulation†

Al Claiborne,*,‡ Joanne I. Yeh,§ T. Conn Mallett,‡ James Luba,‡ Edward J. Crane, III,‡,|| Véronique Charrier,‡ and Derek Parsonage‡

Department of Biochemistry, Wake Forest University Medical Center, Winston-Salem, North Carolina 27157, and Department of Molecular Biology, Cell Biology, and Biochemistry, Brown University, Providence, Rhode Island 02912

Received August 30, 1999; Revised Manuscript Received October 8, 1999

ABSTRACT: While it has been known for more than 20 years that unusually stable cysteine-sulfenic acid (Cys-SOH) derivatives can be introduced in selected proteins by mild oxidation, only recently have chemical and crystallographic evidence for functional Cys-SOH been presented with native proteins such as NADH peroxidase and NADH oxidase, nitrile hydratase, and the hORF6 and AhpC peroxiredoxins. In addition, Cys-SOH forms of protein tyrosine phosphatases and glutathione reductase have been suggested to play key roles in the reversible inhibition of these enzymes during tyrosine phosphorylation-dependent signal transduction events and nitrosative stress, respectively. Substantial chemical data have also been presented which implicate Cys-SOH in redox regulation of transcription factors such as Fos and Jun (activator protein-1) and bovine papillomavirus-1 E2 protein. Functionally, the Cys-SOHs in NADH peroxidase, NADH oxidase, and the peroxiredoxins serve as either catalytically essential redox centers or transient intermediates during peroxide reduction. In nitrile hydratase, the active-site Cys-SOH functions in both iron coordination and NO binding but does not play any catalytic redox role. In Fos and Jun and the E2 protein, on the other hand, a key Cys-SH serves as a sensor for intracellular redox status; reversible oxidation to Cys-SOH as proposed inhibits the corresponding DNA binding activity. These functional Cys-SOHs have roles in diverse cellular processes, including signal transduction, oxygen metabolism and the oxidative stress response, and transcriptional regulation, as well as in the industrial production of acrylamide, and their detailed analyses are beginning to provide the chemical foundation necessary for understanding protein-SOH stabilization and function.

The concept of redox regulation has emerged to accommodate a rapidly growing body of evidence indicating that cellular redox status regulates individual aspects of cellular function (*1*). Oxidative and nitrosative stresses can induce signaling pathways subject to redox regulation, and in a 1998 article devoted to the topic of oxidative modifications in nitrosative stress, Stamler and Hausladen (*2*) have proposed a range of Cys-SH modifications that constitute biological signals on one hand and underlie toxicity on the other. Citing a general principle that a more reactive redox modification provides a greater potential for regulatory function, protein disulfides (Cys-SSR; including both cystine and mixed disulfide forms) and protein-sulfenic acids (cysteine-sulfenic acid; Cys-SOH)[1] have both been considered as mediators of

† Work in this laboratory is supported by National Institutes of Health Grant GM-35394 and by National Science Foundation Grant INT-9803674. J.I.Y. and E.J.C. were the recipients of National Research Service Awards DK-09568 and GM-16274, respectively. J.I.Y. also acknowledges the financial support of Dr. Wim G. J. Hol (Department of Biological Structure, University of Washington, Seattle, WA).

* To whom correspondence should be addressed. Telephone: (336) 716-3914. Fax: (336) 716-7671. URL: http://invader.bgsm.wfu.edu/.

‡ Wake Forest University Medical Center.

§ Brown University.

|| Present address: Department of Chemistry, Salisbury State University, Salisbury, MD 21801.

10.1021/bi992025k CCC: $18.00
Published on Web 11/02/1999

Cys-based redox signaling. While acknowledging the extensive chemical, enzymatic, and genetic studies of cysteine-SH function(s) over the years in a wide range of catalytic, structural, and regulatory contexts, the authors concluded that the molecular basis of redox sensitivity in proteins is not well understood. Another interesting prediction that was offered concerns the relative stabilities of Cys-SSR and Cys-SOH; the reactivity scale for Cys-SH modifications that is presented implies that Cys-SOH is more stable than the corresponding disulfide and thus less likely to function in redox regulation. That this in fact is not the case is one of the conclusions of this review, as supported by several independent lines of evidence.

One of the major limitations, of course, in the critical evaluation of such an emerging picture concerns the availability of analytical data regarding the biochemistry of protein-SOHs. When this topic was first reviewed authoritatively by Allison in 1976 (*3*), there were no known examples of naturally occurring, much less functional, Cys-SOHs. By 1993 extensive descriptions of the chemistry of sulfenic acids had appeared (*4*, *5*), focusing on their general instability and high degree of reactivity in solution, and chemical evidence strongly supporting (but not directly proving) the existence of functional Cys-SOHs in the flavoprotein Npx and a handful of other proteins had accumulated (*6*). Now fortunately, coincident with rapid progress in describing the biological aspects of oxidative and nitrosative stress and redox signaling, and facilitated to a significant extent by the technological advances in low-temperature crystallographic data collection, crystal structures and NMR analyses of several functionally relevant protein-SOHs as well as small molecule sulfenic acids are available. Given the role proposed for Cys-SOHs in the biological continuum of signal transduction versus toxicity (*2*), a review focusing on the current chemistry and biochemistry of protein-SOHs should serve a very timely purpose in promoting the critical evaluation of various proposals concerning the molecular basis of redox regulation. At the same time, this provides an opportunity to examine the detailed structural and mechanistic parameters for Cys-SOH involvement in both redox and nonredox modes of enzyme catalysis.

SULFENIC ACID CHEMISTRY

The chemical and physical properties of sulfenic acids have been reviewed authoritatively by Kice (*4*) and by Hogg (*5*), and these and other sources provided the background for an earlier discussion of protein-SOHs (*6*). In summary, a sulfenic acid (RSOH) is the simplest organosulfur oxyacid; in contrast to sulfinic (RSO_2H) and sulfonic (RSO_3H) acids, which are quite often stable compounds, RSOHs are generally very unstable and highly reactive. Spectroscopic evidence supporting the predominance of the divalent sulfur tautomer R-S-OH over the tetravalent "sulfoxide" structure R-S(═O)H has been presented, and a set of steric, electronic, and hydrogen-bonding factors has been described which can, either singly or in combination, confer unusual stability to sulfenic acids in a small number of cases. Dramatic progress toward confirming many of these inferences on RSOH structure and reactivity has come with the crystal structures of three such compounds since 1993; these include the sterically protected Bmt-SOH (*7*) and thiophenetriptycene-8-SOH (*8*) and the water-soluble 4,6-dimethoxy-1,3,5-triazine-2-SOH (*9*). The crystal structure of the stable Bmt-SOH (*7*) clearly shows how the rather rigid and inert all-carbon framework provides a bowl-type structure which effectively prevents both the formation of the symmetrical $(Bmt\text{-}S)_2$ disulfide during synthesis (from Bmt-SOH and Bmt-SH) and the generally favored self-condensation reaction of two Bmt-SOHs, which normally would lead rapidly to the corresponding thiosulfinate, the unavoidable and irreversible fate of most sulfenic acids in solution (*4*). In contrast, the reactivity of Bmt-SOH with other reductants, oxidants, and nucleophiles not subject to this steric constraint is entirely consistent with the results of earlier solution studies with stable sulfenic acids. Bmt-SOH represents a reversible two-electron oxidation state which can be either reduced to the starting thiol or oxidized further to give the sulfinic acid; it also reacts as an electrophile to give unsymmetrical disulfides and sulfenamides with RSH and RNH_2, respectively, and as a nucleophile with methyl propiolate to give the vinyl sulfoxide. The crystal structure of the triazine-2-SOH (*9*) allowed the additional advantage of correlating the structure with its properties in aqueous solution. As determined at 90 K, the structure provided direct evidence for strong intermolecular hydrogen bonding between the two molecules of the observed dimeric unit. The planes of the respective aromatic rings are effectively perpendicular to each other and allow for two strong reciprocating hydrogen bonds between ArSOH and the N1 ring nitrogen across the dimer. When maintained at room temperature under dry N_2, the recrystallized material is stable for several weeks with only minimal decomposition. In alkaline solution (pH 12), the triazine-2-SOH remains stable (as the $Ar\text{-}SO^-$ sulfenate anion) for several days; this is in marked contrast to the instability observed in acidic solution (pH 2). The UV spectral properties distinguishing the anionic $Ar\text{-}SO^-$ and Ar-SOH forms led to the determination of a pK_a value of 5.86 for the SOH moiety, which is comparable to the values determined for 1,3,6-trimethyllumazine-7-SOH (*10*) and 1-methyluracil-4-SOH (*11*). The slightly acidic pK_a and the greater stability of the sulfenate form compared to that of the free acid indicate that intermolecular hydrogen bonding of the type represented in the crystal structure does not contribute to stabilization of the triazine-2-SOH in aqueous solution at pH >7. The predominant contributions of the respective "sulfenyl" R-S-OH structures in each of the three stable sulfenic acids were confirmed by comparing the crystallographic S−O bond lengths (1.620 and 1.622 Å for triazine-2-SOH and thiophenetriptycene-8-SOH, respectively, to 1.679 Å for Bmt-SOH) to those of more than 100 known sulfoxide S═O examples (1.444−1.584 Å; *9*).

[1] Abbreviations: Cys-SOH and Cyo, cysteine-sulfenic acid; Npx, NADH peroxidase; GR, glutathione reductase; Nox, NADH oxidase; EH_2, two-electron-reduced enzyme; FADHOOH, C(4a)-peroxyflavin; GSNO, *S*-nitrosoglutathione; DTT, dithiothreitol; DNIC−$(GSH)_2$, dinitrosyl−diglutathione iron complex; Cyx, cysteine-sulfinic acid; Prx, peroxiredoxin; Trx, thioredoxin; Ahp, alkyl hydroperoxide reductase; NBD-Cl, 7-chloro-4-nitrobenzo-2-oxa-1,3-diazole; DTNB, 5,5′-dithiobis(2-nitrobenzoate); HAP1/Ref-1, human apurinic-apyrimidinic endonuclease/nuclear redox factor; AP-1, activator protein-1; Cys-SNO, *S*-nitrosocysteine; PTP, protein tyrosine phosphatase.

PROTEIN-SULFENIC ACIDS: RULES FOR STABILIZATION

The SOH functionality of Bmt-SOH is surrounded by a protective molecular cavity (*7*), and Liu has suggested (*12*) that the stability of Cys-SOH in proteins is similarly derived from limited solvent access, possibly in association with an apolar microenvironment. Bmt-SOH reacts readily with thiols to form disulfides, and Allison has concluded (*3*) that the absence of proximal Cys-SH groups is a primary factor in providing for the formation of stable Cys-SOH. In addition to the influence of hydrogen bonding and/or ionization of SOH to the sulfenate form, as described above with the triazine-2-SOH system (*9*), these factors represent a set of criteria for the appropriate, and perhaps unusual, protein microenvironment required for Cys-SOH stabilization. In 1996, Yeh et al. (*13*) published the refined 2.8 Å structure of the flavoprotein Npx as determined under cryogenic conditions; this work allowed the first structural evaluation of an essential Cys-SOH (Cys42-SOH) in its native state, albeit at medium resolution. In addition to the four new high-resolution crystal structures now available for functionally relevant protein-SOHs, very strong chemical evidence supports similar structures in at least five other proteins; for the purpose of the following discussion, these individual examples of Cys-SOH involvement have been grouped into four overlapping categories: (1) FAD-dependent peroxide and disulfide reductases, (2) NO-inhibition mechanisms, (3) peroxiredoxins, phosphatases, and signal transduction, and (4) redox regulation of transcription factor signaling.

FAD-DEPENDENT PEROXIDE AND DISULFIDE REDUCTASES

The pyridine nucleotide-disulfide oxidoreductase family was originally defined as a group of functionally related dimeric flavoenzymes containing one FAD and one redox-active disulfide per subunit; GR is the prototype of one predominant disulfide reductase class (*14*). Subsequent structural studies of *Enterococcus faecalis* Npx demonstrated that, although the enzyme does not contain a redox-active cystine, it is a close structural homologue of GR (*15*). The extensive structural homology between Npx and Nox ($O_2 \rightarrow 2H_2O$), combined with their detailed mechanistic similarities, has led these two enzymes to be termed peroxide reductases (*6*, *16*). It is important to emphasize that while GR and other members of its class have functionally distinct interchange and charge-transfer thiols in their respective two-electron-reduced (EH_2) forms (*14*), Npx and Nox preserve only the latter Cys equivalent; this Cys-SH (in the EH_2 intermediate) is also directly involved in the respective peroxide reduction reaction (*17*, *18*).

NADH Peroxidase. Since 1996, both crystallographic (*13*) and NMR (*19*) analyses of the fully active, native oxidized Cys42-SOH and reduced Cys42-SH forms of Npx have become available. The original 2.8 Å structure of Cys42-SOH Npx has recently been improved[2] to 2.1 Å, allowing a much more detailed view of the active site and the Cys42-SOH environment (Figure 1); in both cases, data collection at 110 K was necessary to stabilize the Cys-SOH. The

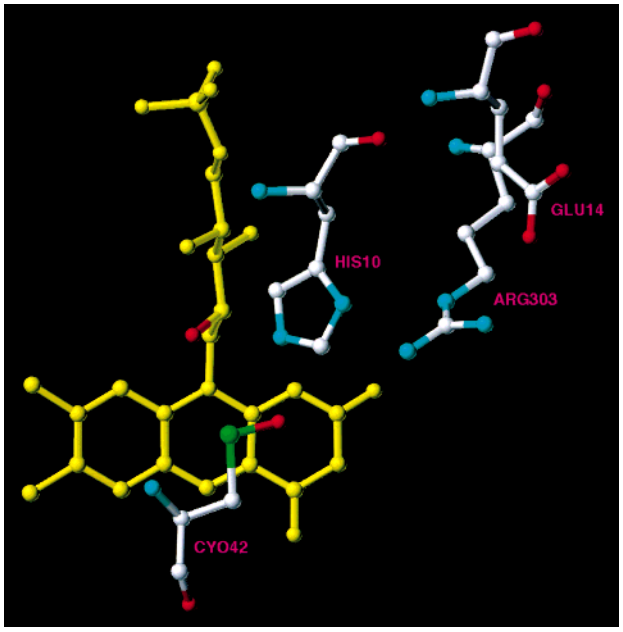

FIGURE 1: Active site of the wild-type Npx Cys42-SOH form from the refined 2.1 Å crystal structure. Cyo42 O_δ is hydrogen bonded to His10 $N_{\epsilon 2}$ and FAD O2′ (red), and Cyo42 S_γ has similar interactions with Cyo42 N and FAD O2′. Other details are given in the text.

structure shows that Cys42-SOH (Cyo42) atoms C_α, C_β, S_γ, and O_δ define a planar arrangement which is essentially parallel to the plane of the flavin; this positions Cyo42 S_γ 3.6 Å from FAD C(4a), while Cyo42 O_δ is located 3.3−3.5 Å from FAD C(10a), N(1), and C(4a). Active-site stabilization of Cys42-SOH appears to derive from the resulting electronic interaction between the Cyo42-SO function and the electron-deficient flavin, very limited solvent access, and weak interactions between Cyo42 O_δ and both FAD O2′ (3.5 Å) and His10 $N_{\epsilon 2}$ (3.4 Å). Arg303 N_ϵ is hydrogen-bonded (3.0 Å) to the active-site His10 $N_{\delta 1}$, thus maintaining the imidazole side chain in a neutral protonation state (*20*); as a consequence, this relatively strong interaction stabilizes the His10 $N_{\epsilon 2}$(H) tautomer. Given the likelihood that His10 is thus a weak hydrogen bond donor to Cyo42 O_δ, and taken together with the weak charge-transfer interaction indicated previously for Cys42-SOH and the flavin in oxidized wild-type Npx (*21*), it is also likely that the native oxidized Npx environment stabilizes the Cys42-SO^- sulfenate species. This is also consistent with the well-documented requirement for Cys-S^- thiolate (not Cys-SH) in the charge-transfer interaction observed in the EH_2 forms of Npx and GR (*14*). When it is considered that in aqueous solution the sulfenate forms of the triazine-2-SOH and some other sulfenic acids (*10*, *11*) are preferentially stabilized, and given the fact that Cys42 is the only Cys residue in Npx, the native peroxidase structure indicates that all four of the criteria for Cys-SOH stabilization by the protein microenvironment are fulfilled.

The suboptimal hydrogen-bonding interaction indicated for His10 $N_{\epsilon 2}$(H) and Cys42-SO^- raises a further interesting question about His10 and the active-site environment of Cys42-SOH. Mutagenesis studies (*22*) have shown that, while His10 is not essential for catalytic activity, its replacement (H10Q or H10A) leads to a 50−70-fold increase in $K_m(H_2O_2)$ at pH 7.0, where the wild-type Npx EH_2 Cys42-SH is fully ionized ($pK_a \leq 4.5$). While the H10Q mutation

[2] J. I. Yeh, E. J. Crane, III, D. Parsonage, and A. Claiborne, manuscript in preparation.

appears to have no effect on this pK_a, it does lead to a dramatic 160-fold decrease in the second-order rate constant (from 3.0×10^6 to 1.9×10^4 M^{-1} s^{-1}) for the formation of Cys42-SOH from EH_2 and H_2O_2 at pH 7.0 and 5 °C. This result quantitatively accounts for the observed increase in $K_m(H_2O_2)$ and has been interpreted in terms of a hydrogen-bonding interaction between His10 $N_{\epsilon 2}$(H) and the peroxide oxygen(s) during the nucleophilic attack of Cys42-S^- on H_2O_2. This stabilizes the transition state by some 2.8 kcal/mol and is a critical factor in the rate of Cys42-SOH formation. Further evidence supporting the significance of the interaction between His10 and Cys42-SOH comes from analyses of the oxidized H10Q mutant. Replacement of His10 with Gln leads to a strong enhancement of the charge-transfer interaction between Cys42-SOH and the flavin; a well-defined absorbance band centered at $\lambda_{max} = 650$ nm now appears. As expected, reduction of Cys42-SOH → Cys42-SH can be monitored by the decrease in A_{650}, and the process is reversed with H_2O_2. At the same time, oxidation of Cys42-SOH with excess H_2O_2 leads to irreversible loss of the 650 nm band with the H10Q mutant; kinetic analyses demonstrate that the second-order rate constant for this process, which primarily involves oxidation of Cys42-SOH to Cys42-SO_2H, is 50-fold faster with the mutant than with wild-type Npx. This result has been interpreted in terms of the His10 $N_{\epsilon 2}$-(H) hydrogen-bonding interaction seen in the 2.1 Å crystal structure of the wild-type enzyme, which stabilizes the Cys42-SOH ground state by 2.3 kcal/mol and thus decreases the rate of H_2O_2 oxidation to Cys42-SO_2H. Again, the enhanced Cys42-SOH → FAD charge-transfer absorbance in H10Q Npx, taken together with the requirement for the anionic form of the Cys42 charge-transfer donor as discussed previously, strongly supports active-site stabilization of the Cys42-SO^- species. The 650 nm absorbance band shows no pH-dependent intensity decrease at pH 5.4, so it appears that the corresponding pK_a is $\leq$4.5.

The crystal structure of the native oxidized H10Q mutant has recently been refined[2] at 2.4 Å; comparison with the wild-type structure reveals two significant active-site conformational changes. There is a major change in the side chain conformation of Arg303 which flips the guanidinium moiety and causes a 1.3 Å displacement of C_δ. There is also a more subtle shift in the side chain conformation of Cys42-SOH which has the net effect of decreasing the distance between Cyo42 S_γ and the electron-deficient isoalloxazine ring system of FAD. In particular, the sulfur atom is now only 3.2 Å from FAD C(4a), comparable to the separation of 3.3 Å observed between Cys63 S_γ and FAD C(4a) in the structure of the GR EH_2 charge-transfer intermediate (*23*), and we conclude that the enhanced charge-transfer interaction in oxidized H10Q Npx is largely due to this movement of Cyo42 S_γ. As in the wild-type structure, Cyo42 S_γ is also positioned to receive hydrogen bonds from FAD O2′ (3.3 Å) and Cyo42 N (2.9 Å); there is a single significant interaction with Cyo42 O_δ, which receives a hydrogen bond from Gln10 $N_{\epsilon 2}$ (3.0 Å). It is also worth noting that the Cyo42 $C_\beta-S_\gamma$ bond lengths (1.8 Å) in these two Npx structures compare very favorably with those of the C−S bonds in the three stable sulfenic acid structures mentioned previously (1.731−1.833 Å), as do the $C_\beta-S_\gamma-O_\delta$ bond angles of 99−102° (vs 100−103° in the small molecule structures). Although limited by the resolution of the protein structures, it is interesting to note that the Cyo42 $S_\gamma-O_\delta$ bond lengths of 1.4 Å compare more favorably with those of small molecule sulfoxides (S═O; 1.444−1.584 Å) than with those of the three stable sulfenic acids (1.620−1.679 Å). If this analysis is taken literally, and given the stabilization of Cys42-SO^- indicated by the Npx structures, it could suggest considerable S═O character within the Cys42-sulfenate and localize the negative charge to Cyo42 S_γ [CH_2-S(═O)$^-$].

NMR studies of [3-^{13}C]Cys-labeled Npx (*19*) allowed the first analysis of a protein-SOH and also documented the change in chemical shift on reduction of Cys42-SOH → Cys42-SH in wild-type Npx. Difference ^{13}C NMR spectra of Cys42-SOH minus Cys42-SH forms of Npx at pH 7.0 therefore gave a maximum at 41.3 ppm and a minimum at 30.8 ppm, corresponding to the oxidized and reduced forms of Cys42, respectively. H_2O_2 oxidation of Cys42-SOH, which led primarily to the formation of Cys42-SO_2H as determined by mass spectrometry, was accompanied by the loss of the 41.3 ppm resonance as a new maximum appeared at 57.0 ppm. The 3-^{13}C chemical shift for Cys42-SH was found to compare favorably with those reported for other protein-SH, while the values for Cys42-SOH and Cys42-SO_2H were evaluated on the basis of chemical shifts calculated for neutral, oxidized derivatives of Cys-SH. The calculated Cys-SOH and Cys-SO_2H shifts of 39.6 and 58.8 ppm, respectively, were in good agreement with the experimental values for Cys42-SOH (41.3 ppm) and Cys42-SO_2H (57.0 ppm); the overall $\Delta\delta$ of 26.2 ppm for oxidation of Npx Cys42-SH → Cys42-SO_2H is comparable to the $\Delta\delta$ of 24.3 ppm measured for free Cys-SH and Cys-SO_2H[3] at pH 7.5−7.7. Baleja and colleagues (*24*) have recently reported a [3-^{13}C]-Cys chemical shift of 26.9 ppm for reduced Cys340-SH (pH 5.8) in the recombinant DNA-binding domain of the bovine papillomavirus-1 E2 protein; Cys340 has also been proposed to cycle between SOH and SH states during redox regulation of E2 DNA binding (*25*).

NADH Oxidase. Mallett et al. (*26*) have shown that the C42S mutant (*E. faecalis* Nox) is reduced directly with only 1 equiv of NADH (as opposed to 1.5−1.7 equiv for wild-type Nox), which supports the existence of a Cys42-SOH redox center as proposed originally (*27*). A refined 2.5 Å crystal structure is now available for the analogous C44S mutant of the Nox from *Streptococcus pyogenes*,[4] and a 1.82 Å synchrotron data set has been collected for the wild-type enzyme. As interpretations of these structural data are still in progress, we will review the kinetic and redox properties of *E. faecalis* Nox relative to the Cys-SOH redox center, with specific reference to Npx. The dimeric forms of both wild-type and C42S Nox exhibit active-site asymmetry as revealed in their respective redox and kinetic properties; a surprising feature is that one Cys42-SOH in the wild-type enzyme is not reduced directly with either NADH or dithionite in static titrations (*26*). Given the generally high reactivity of sulfenic acids, this suggests a conformational nonequivalence between the two active sites per dimer which moves Cys42-SOH away from the flavin and eliminates the possibility of reduction by E−$FADH_2$·NAD^+. A similar situation was observed in the Npx L40C mutant, which forms

[3] J. Baleja, personal communication.

[4] T. C. Mallett, H. Sakai, D. Parsonage, A. Claiborne, and T. Tsukihara, manuscript in preparation.

a new Cys40−Cys42 disulfide; the crystal structure shows that Cys42 S_γ is moved to a new position 5.9 Å from FAD C(4a), preventing electron transfer from E−$FADH_2$·NAD^+ (*28*). Further equilibrium analyses of wild-type Nox have suggested that the nonproductive conformation may be influenced by bound NAD^+, however, so as to provide for the normal four-electron reduction of $O_2 \rightarrow 2H_2O$ at both active sites during turnover, in an asymmetric mechanism. A second interesting feature regarding the Cys-SOH redox center in Nox concerns the presence of Cys-SOH → FAD charge-transfer interactions, which are most prominent in the visible absorbance spectra of the enzymes from *Streptococcus mutans* and *Streptococcus pneumoniae*.[5] In both cases, distinct bands with $\lambda_{max} \sim 600$ nm are observed, similar to that in H10Q Npx, and reduction can be monitored by the isosbestic conversion to an EH_2 charge-transfer intermediate ($\lambda_{max} \sim 530$ nm). We can conclude that these Cys-SOH → FAD charge-transfer interactions specifically reflect the "productive" active-site conformation within the respective asymmetric Nox dimer (*26*). All five Nox sequences from enterococci, streptococci, and lactococci show that Npx His10 is absolutely conserved; it is likely that His10 interacts with and stabilizes Cys-SOH as seen in Npx.

The stoichiometry of O_2 reduction catalyzed by C42S Nox is altered dramatically, in that H_2O_2 is now produced in turnover (*18*). The fact that wild-type Nox carries out the fully coupled reduction of $O_2 \rightarrow 2H_2O$ strongly supports the conclusion that Cys42-SOH/-SH in Nox functions as a peroxidatic center, directly analogous to its catalytic role in Npx. Furthermore, kinetic studies of C42S Nox have shown that (1) the E−$FADH_2$·NAD^+ complex is the O_2-reactive species in turnover and (2) the rapid O_2 reaction leads to the formation of an FAD C(4a)-hydroperoxide as the primary oxygenated Nox intermediate. In the C42S mutant, H_2O_2 is eliminated directly to give E−FAD at 35 s^{-1}. In the structure of C44S Nox from *S. pyogenes*,[4] Ser44 O_γ is located on the *si* face of the flavin opposite from the NAD^+-binding site; this would put Cys44 S_γ of the wild-type enzyme in a very favorable position (in the EH_2−FADHOOH intermediate) for nucleophilic attack on the distal peroxyflavin oxygen, yielding the oxidized Cys44-SOH and the C(4a)-hydroxyflavin. The latter species can eliminate H_2O directly to give E−FAD. While the details of His10 involvement in Nox catalysis await studies with the appropriate mutants, there is one very important difference in the active-site structures of Nox and Npx. Arg303, which has important interactions with His10 in Npx as described previously, is replaced with Val314 in the *S. pyogenes* C44S Nox; Val314 is conserved in all five Nox sequences as either Val or Leu.

NO-INHIBITION MECHANISMS

GSNO-Inhibited Glutathione Reductase. Nitric oxide (NO) has been described as a pluripotent regulatory molecule (*29*); as such, it is involved in a multitude of cellular signaling pathways. Excessive or uncontrolled nitrosylation, however, can lead to the loss of cellular function, thus giving rise to the condition termed "nitrosative stress". Due to the short half-life of 0.1 s for authentic NO in vivo, the existence of longer-lived physiologic NO carriers has been proposed (*30*), and Hausladen et al. (*31*) have shown that GSH is the major NO group acceptor in *Escherichia coli*. In 1995, Becker et al. (*30*) showed that purified human GR was inhibited by GSNO in the presence of NADPH; originally this effect was characterized as an irreversible inhibition, since incubation with 5 mM DTT for 30 min gave only slight reactivation. Nitrosylation of Cys63 and/or Cys58 (which together form the GR redox-active disulfide; see above) was considered as the likely cause of this "irreversible" inhibition by GSNO. More recently, however, it was shown (*29*) that full reactivation of GSNO-inhibited GR could be achieved with a 24 h incubation in the presence of 5 mM DTT. In addition, the 1.7 Å crystal structure of GSNO−GR (*29*) clearly demonstrates that inhibition does not involve nitrosylation of either active-site Cys; instead, Cys63-SH is oxidized to Cys63-SOH, and Cys58-SH forms a mixed disulfide with GSH. Furthermore, Cyo63 represents an unusually stable example of a protein-SOH, in that crystallographic data collection under aerobic conditions at ambient temperature allowed the unequivocal demonstration of the Cys63-SOH structure. A synchrotron data set collected under cryogenic conditions extended the resolution to 1.4 Å and gave the same Cys63-SOH structure; when GSNO-GR crystals were soaked for 24 h with 10 mM DTT, followed by back-soaks without DTT, X-ray analysis at 2.0 Å showed complete removal of the GSH moiety from Cys58, and formation of the Cys58−Cys63 disulfide was evident in a large proportion of the GR molecules. These results are consistent with the slow DTT reactivation of GSNO−GR observed in solution. The modifications at both protein-SHs support the requirement for NADPH in GSNO inhibition; oxidized GR, which is not inhibited by GSNO (*30*), must be reduced to the EH_2 form prior to reacting with the NO carrier. The modification of Cys63-SH (the charge-transfer thiol) explains the absence of EH_2 charge-transfer absorbance in the modified enzyme.

Apart from the modifications of the two Cys residues, only small shifts were observed for native active-site atoms when the GSNO−GR structure was compared with that for native GR. Cyo63 O_δ forms strong hydrogen bonds with Cyo63 N (2.8 Å) and FAD O2′ (2.8 Å) and a weaker interaction with Thr339 O_γ (3.2 Å); Cyo63 S_γ remains in van der Waals contact with the flavin [3.3 Å from FAD C(4a)], although the Cys → FAD charge-transfer interaction is absent. There is no direct evidence regarding the Cys63-SOH ionization state, although the active-site environment of GR is known to stabilize the Cys63-thiolate ($pK_a \leq 5$) in the EH_2 form. With regard to the other two criteria for protein-SOH stabilization, Cys63 is located in a buried pocket within the active site which provides very restricted solvent access to Cys63-SOH, and the proximal Cys58 $S\gamma$ is involved in the mixed disulfide with GSH, preventing its reaction with Cys63-SOH to form the redox-active cystine. Although the reaction sequence leading from the initial interaction between the GR EH_2 form and GSNO to the oxidation of Cys63 is not known, Becker and colleagues (*32*) have also shown that GR is irreversibly inactivated by a second in vivo NO carrier, DNIC−$(GSH)_2$. The 1.7 Å crystal structure of the resulting GR derivative (*29*) clearly shows that Cys63 is now oxidized (irreversibly) to Cys63-SO_2H. There is at least one recent report indicating that either endogenous NO or incubation with NO carriers such as GSNO inhibits GR in macrophages (*33*), and these in vitro studies with purified GR certainly

[5] D. Parsonage, T. C. Mallett, and A. Claiborne, unpublished results.

support the general conclusion that oxidative modifications of protein-SH must be considered in addition to nitrosylation in the analysis of molecular mechanisms for both NO-based redox signaling and nitrosative stress.

NO-Inhibited Nitrile Hydratase. As indicated above, the evaluation of longer-lived physiologic NO carriers has focused on cellular thiols such as GSH and on transition metals such as iron. Nitrile hydratase from *Rhodococcus* sp. N-771 is a non-heme iron(III) enzyme which catalyzes the production of amides via hydration of the corresponding nitriles (*34*); the worldwide application of such Fe-type and Co-type nitrile hydratases accounts for the industrial production of some 30 000 tons of acrylamide per year (*35*). The enzyme from *Rhodococcus* sp. N-771 exhibits an unusual photosensitivity in vivo; aerobic incubation of cells in the dark leads to the reversible loss of activity, and this can be restored by light irradiation. Spectroscopic investigations into the mechanism of this dark inactivation/photoactivation cycle have shown that association of the iron center with endogenous NO causes the inhibition (*36*); photodissociation of this NO activates the enzyme on exposure to light. While the physiological significance of this NO inhibition cycle is not known, it has been cited as the first example of NO regulation of an enzyme activity in bacteria (*34*). This nitrile hydratase is an $(\alpha\beta)_2$ heterotetramer (*37*); the iron center is associated specifically with the α subunit, and the active site is at the $\alpha-\beta$ interface within the respective heterodimeric unit. The application of a variety of spectroscopic approaches, including extended X-ray absorption fine structure, had implicated S, N, and O ligands within the iron center, and mass spectrometric analyses (under acidic conditions) of the limiting 11-residue peptide (from the α subunit) required for the NO−iron center revealed that Cys112 is oxidized post-translationally to Cys112-SO_2H (*38*). In 1998, the 1.7 Å crystal structure of the NO−nitrile hydratase complex was reported (*34*), as determined with synchrotron radiation in the dark at room temperature. In addition to identifying the iron center ligands and the mode of NO binding, these results confirmed the Cys112-SO_2H structure for α-Cys112 and also established that α-Cys114 had been modified post-translationally to give Cys114-SOH. The S_γ atoms of α-Cys109-SH, Cys112-SO_2H, and Cys114-SOH are all ligands to Fe(III) (2.3 Å), as are the main chain N atoms of α-Ser113 and Cyo114 (2.1 Å). The Fe−N bond length for the nitrosyl iron is 1.7 Å, and the O atoms contributed by Ser113 O_γ, Cyx112 $O_{\delta1}$, and Cyo114 O_δ have been described as forming a claw setting that holds the NO molecule tightly in place above the plane of the iron center. The respective O−N and O−O distances are 2.7−3.3 Å; it has been suggested that the process of photoactivation involves initial disruption of the Fe−NO bond followed by a localized structural change within the claw setting which weakens the NO interaction further.

To confirm the modified Cyx112 and Cyo114 structures, mass spectrometric analyses of the limiting tryptic peptide containing the iron center were carried out under neutral as well as acidic conditions; these results fully support the assignments of the two modified Cys residues in the crystal structure. The SOH and SO_2H moieties of Cyo114 and Cyx112 interact strongly (2.7−3.2 Å) with the guanidinium nitrogens of Arg56 and Arg141 from the β subunit, suggesting that both Cys114-SOH and the strongly acidic Cys112-SO_2H are stabilized as the respective sulfenate and sulfinate anions. These Arg residues are conserved in all known nitrile hydratases, and their replacement by mutagenesis leads to the loss of enzyme activity as well as changes in the visible absorbance spectrum reflecting the electronic state of the iron center. This provides a further rationale for the functional significance of the Cys112 and Cys114 post-translational oxidations, in terms of stabilizing the active site at the subunit interface in concert with these Arg residues. In the NO complex, of course, Cys114-SOH is also stabilized through the interaction of O_δ with the NO molecule. Although Cys109 shares the same active site with Cyo114, the interatomic (S_γ) distance, their respective interactions with the iron, and geometric factors prevent any direct interaction between them. With regard to the mechanism(s) involved in the post-translational modifications of Cys112 and Cys114, it has recently been demonstrated (*39*) that successful overexpression of the fully active recombinant nitrile hydratase in *E. coli* requires coexpression of the nitrile hydratase activator protein; this soluble protein appears to act catalytically and may be involved in either the incorporation of iron or possibly the post-translational modifications of Cys112 and Cys114. Furthermore, chemical modification and mass spectrometric and sequence analyses of the respective active-site peptides were performed for the α subunit from the fully active, soluble recombinant enzyme and from the insoluble inclusion bodies that resulted on expression in the absence of the activator protein. Only the fully active nitrile hydratase containing the correctly formed iron center also contained the Cys112-SO_2H modification; there was no similar (irreversible) oxidation of Cys112 in the absence of the functional iron center. Indirect evidence from the mass spectrometric analysis suggests the presence of Cys114-SOH in the fully active recombinant enzyme as well.

Mechanistically, the direct involvement of NO in these Cys oxidations seems to be excluded by the fact that, although *E. coli* does not produce endogenous NO, the recombinant nitrile hydratase still contains Cys112-SO_2H. A more likely mechanism under consideration involves a self-oxygenating process in which the functional non-heme iron center catalyzes the modification, although a possible role for the activator protein in this regard cannot be ruled out. All four active-site residues participating in the iron center (Cys109, Cys112, Ser113, and Cys114) are conserved not only in the Co-type nitrile hydratases but also in the thiocyanate hydrolase from *Thiobacillus thioparus* THI 115 (*40*). These observations suggest that the coordination spheres within the active centers of these three types of functionally related enzymes may be very similar and may also exhibit post-translational oxidations of the Cys residues that are involved (*37*).

It should also be mentioned, in the context of Cys-SOH involvement in NO-inhibition mechanisms, that DeMaster et al. (*41*) have shown that under anaerobic conditions 2 mol of NO reacts with Cys34-SH of human serum albumin to yield the Cys34-SOH derivative and nitrous oxide (N_2O).

PEROXIREDOXINS, PHOSPHATASES, AND SIGNAL TRANSDUCTION

As has been reviewed recently by Denu and Dixon (*42*) and by Nakamura et al. (*1*), cellular redox status plays an

important role in the mechanisms that regulate the activities of growth factors and tyrosine phosphorylation-dependent signal transduction pathways and other aspects of cellular function. H_2O_2 has been described as stimulating a complete program of mitogenic signal transduction, and it has also been shown that H_2O_2 is generated transiently during growth factor stimulation (*42*). The src family protein tyrosine kinase Lck, for example, becomes heavily tyrosine-phosphorylated when T-cells are incubated with H_2O_2 (or with diamide), and this response has been attributed to inhibition of protein tyrosine phosphatase(s) (*1*). Another major regulatory factor in these and other H_2O_2-dependent signaling pathways is provided by the Prxs, which constitute a recently identified cysteine peroxidase family (*43*, *44*) and are abundant in the cytosol of most mammalian tissues; these enzymes are capable of reducing the H_2O_2 produced transiently during growth factor stimulation, for example (*45*). It has now been shown that at least one such Prx can also interact directly with signaling components, offering an additional regulatory mechanism (*46*).

The hORF6 Peroxiredoxin. There are two major Prx classes which are distributed over the three phylogenetic kingdoms, and the primary distinction is based on the presence of either a single redox-active Cys or intersubunit disulfide in the active site (*44*). hORF6 is a one-Cys Prx that reduces $H_2O_2 \rightarrow 2H_2O$ with electrons supplied by an unidentified cellular thiol that is not Trx or GSH (*47*). Cys47 is the site of H_2O_2 reduction, since the C47S mutant lacks peroxidase activity, and a Cys47-SOH intermediate has been proposed in the catalytic redox cycle (with DTT as the reducing substrate). In 1998, the 2.0 Å structure of the hORF6 C91S mutant was determined (*45*) with data collected at room temperature using an in-house X-ray source. The protein exists as a tightly bound dimer of ~25 kDa subunits; in the two-Cys Prxs, the redox-active disulfide involves Cys47 and Cys170′ (yeast Trx peroxidase; *48*). In distinct contrast, the hORF6 structure clearly presents Cys47 in the stable SOH form. The only other Cys residue in wild-type hORF6 is Cys91, but earlier studies demonstrated the complete absence of any disulfide (intra- or intermolecular) in the native protein (*47*); the C91S structure gives an interatomic (C_α) distance of ~17 Å between Cyo47 and Ser91. Cyo47 is located within a segment (Phe43−Glu50) of domain I which interacts with domain II′; a narrow active-site pocket formed by residues from these complementary domains restricts solvent access to Cys47-SOH, which is located at the bottom of the pocket. There are suggestions from the active-site structure concerning additional modes of Cys47-SOH stabilization as well as the catalytic mechanism. In particular, His39 $N_{\delta 1}$ is positioned to interact with Cyo47 S_δ (3.0 Å), and a catalytic role in stabilizing Cys47-S^- in reduced hORF6 has been proposed; this His is replaced by Tyr44 in the structure of a two-Cys Prx (HBP23/PAG), however, despite the fact that the conserved Cys52 still functions as the H_2O_2 reaction center (*46*). Arg132 $N_{\eta 1}$ in hORF6 is 3.7 Å from Cyo47 S_γ, but the closest approach between the conserved Arg128 and Cys52 S_γ in oxidized HBP23 is 7.4 Å. Significant local structural changes have been implicated in the reaction mechanism proposed for the two-Cys Prx (*46*), and similar shifts in the reduced hORF6 structure might also be necessary to fully explain the reactivity of Cys47-SH with H_2O_2. One potential stabilizing interaction described for Cyo47 O_δ involves a possible Mg(II) ion at 3.5 Å, but the significance of this bound Mg relative to the solution properties of hORF6 is unclear.

The AhpC Peroxiredoxin. While hORF6 and HBP23 are mammalian one- and two-Cys Prxs which accept electrons from an unidentified cellular thiol and from Trx, respectively, AhpC from *Salmonella typhimurium* is a two-Cys Prx that is reduced by the NADH-dependent AhpF flavoprotein component (*49*). The Cys46−Cys165′ redox-active disulfide, other than differing in its specificity for reducing substrate, is functionally equivalent to those of HBP23 and yeast Trx peroxidase, for example. Somewhat surprisingly, the C165S mutant is fully active in steady-state assays including AhpF, NADH, and cumene hydroperoxide (*50*); the C46S mutant on the other hand has no activity and can be compared directly with the C47S mutant of hORF6. Spectral titrations have shown that incubation of C165S AhpC with 1 equiv of H_2O_2 leads to the generation of an AhpC intermediate which is reduced by AhpF and 1 equiv of NADH; the C46S mutant does not form the analogous oxidized derivative of Cys165 even with a 100-fold excess of H_2O_2. In a subsequent study, Ellis and Poole (*51*) demonstrated that the oxidized C165S AhpC species reacted with the NH_2 and SH reagent NBD-Cl (formerly Nbf-Cl; *52*) to give a product that could easily be distinguished from the Cys46-S−NBD adduct by either fluorescence or absorbance; mass spectrometric analyses demonstrated very clearly that the adduct formed from the oxidized AhpC mutant gave an increase of 16 Da (one oxygen) over the thiol adduct. Thus, oxidation of Cys46-SH with 1 equiv of H_2O_2 leads to the stable formation of Cys46-SOH in the C165S mutant, and Cyo46 reacts as a nucleophile with NBD-Cl. While the analyses presented did not allow the conclusive determination of sulfoxide versus sulfenate ester structures for the Cyo46−NBD adduct, Ellis and Poole (*51*) have taken the former to be most likely; this is also consistent with the stability of the adduct as observed under the acidic conditions of the mass spectrometric analyses and indicates that Cyo46 S_γ is the nucleophilic center in the reaction. Cys46-SOH has also been shown to react with 2-nitro-5-thiobenzoate to give the mixed disulfide (*50*), indicating that the SOH moiety can behave as an electrophile under appropriate conditions.

Several important conclusions regarding SOH stabilization and reactivity emerge from these and other AhpC studies. For one thing, the mutant Cys46-SOH is reduced to Cys46-SH by AhpF at a rate that is fast enough to support the wild-type turnover number. The chemical and kinetic analyses of the Cys46-SOH/-SH redox center clearly show that the protein microenvironment is a major factor in promoting the reactivity of Cys46-SH (not Cys165) with H_2O_2; on the other hand, comparisons of DTNB reaction rates for Cys46 and Cys165 reveal quite similar kinetic behavior (*50*), so simple solvent accessibility is not a significant determinant. And, since the AhpC C165S mutant is the functional equivalent of hORF6 with regard to Cys-SOH stabilization and catalytic H_2O_2 reduction, these studies complement the hORF6 structure very nicely. The very recent structure of the Cys52−Cys173′ disulfide form of HBP23 has led to the suggestion (*46*) that in the reduced enzyme Cys52-SH may approach the two conserved active-site Arg residues (Arg128 and Arg151) and thus enhance both its accessibility and its reactivity with H_2O_2; the resulting Cys52-SOH then reacts

rapidly with Cys173′-SH to reform the disulfide. The same mechanism has been proposed by Ellis and Poole for Cys46 and Cys165′ in the wild-type AhpC peroxidatic cycle (*50*).

H_2O_2-Inhibited Protein Tyrosine Phosphatases. Recently, Denu and Tanner (*53*) have demonstrated that purified protein tyrosine phosphatases such as VHR and PTP1 are readily inhibited by H_2O_2; inhibition is largely reversible with either GSH or DTT. The competitive inhibitor phosphate protected both VHR and PTP1 from H_2O_2 inactivation; this result, combined with the demonstration that H_2O_2-inhibited VHR no longer reacts with iodoacetate, strongly supported the conclusion that the catalytic Cys124-SH was the target of H_2O_2 inactivation. The possibility that this modification resulted in a stable Cys124-SOH derivative was tested directly by comparing the spectral properties of the VHR−NBD adducts obtained with and without H_2O_2 preincubation. While the clarity of the spectral data does not compare to that reported for the AhpC Cys46−NBD derivatives (*51*), H_2O_2 treatment of VHR still led to at least partial formation of Cys124-SOH, as taken from the difference spectrum ($\Delta A_{max} \sim 345$ nm, $\Delta A_{min} \sim 430$ nm) for the NBD adducts obtained with H_2O_2-treated and untreated VHR, respectively. Although NBD labeling of wild-type VHR was substoichiometric (about 0.5 NBD/VHR polypeptide), parallel experiments with the C124S mutant did clearly indicate the absence of any such change in the NBD adduct spectrum ($\lambda_{max} =$ 420 nm; three Cys residues remain in the VHR mutant) of the H_2O_2-treated protein. Chemical modification approaches have also been taken to implicate the SOH derivative of the catalytic Cys215 in the reversible H_2O_2 inactivation of PTP1B (*54*), and growth factor stimulation of cultured cells led to a time-dependent change in the distribution between Cys215-SH and presumed Cys215-SOH forms of the enzyme in vivo as well. The Trx system (Trx, Trx reductase, and NADPH) was shown to reactivate H_2O_2-inhibited PTP1B in vitro, presumably by reduction of Cys215-SOH → Cys215-SH. Taken together with the physiological roles ascribed to the cytosolic Prxs in H_2O_2 elimination and, in the case of HBP23/PAG, specific protein tyrosine kinase inhibition, a regulatory scheme accounting for the overall role of H_2O_2 in tyrosine phosphorylation-dependent signaling pathways in vivo has begun to emerge.

REDOX REGULATION OF TRANSCRIPTION FACTOR SIGNALING

Fos and Jun, HAP1/Ref-1, and the E2 Protein. The chemical evidence for redox regulation of Fos and Jun (AP-1) and bovine papillomavirus-1 E2 protein and, more specifically, for the involvement of Cys-SOH/-SH redox cycles in the regulation of the respective DNA target binding, has been reviewed previously (*6*, *55*). Recently, a major focus regarding AP-1 redox regulation (reductions of Fos Cys154-SOH and Jun Cys272-SOH, as proposed) has involved the structure and function of HAP1/Ref-1 (*56*−*58*), the bifunctional nuclear protein that stimulates AP-1 DNA binding through a redox cycle that involves Trx. Although Cys65 is clearly implicated in Ref-1 redox activity, both the structure of the Ref-1 redox center and the mechanism by which it reduces AP-1 remain to be elucidated. In 1992, Hegde et al. (*59*) reported the 1.7 Å structure of the complex between the E2 DNA-binding domain, which includes Cys340, and its DNA target. The DNA-binding specificity ($K_d = 0.4$ nM) derives primarily from direct interactions involving four of the conserved amino acids within the recognition helix. Among these, Cys340 is involved in two hydrogen-bonding interactions, each of which is mediated between S_γ and the respective base. As seen with the Fos-C154S/Jun-C272S mutant heterodimer, the E2 C340S mutant still binds its DNA target; estimates of binding affinities, however, indicate that the Ser substitution weakens the interaction by a factor of about 2, while the C340A mutant binds DNA with only ≤10% of the wild-type affinity (*25*). The proposal that oxidation of E2 Cys340-SH → E2 Cys340-SOH represents the molecular basis for in vitro redox regulation of DNA binding is consistent with the structural data, although again direct and definitive proof remains elusive.

Nuclear Factor I. The evidence for redox regulation of nuclear factor I (*60*) and a possible role for a Cys3-SOH/-SH cycle in this capacity is similar to that reviewed earlier for Fos, Jun, and the E2 protein. However, the DNA-binding domains of all nuclear factor I family members contain not one but four conserved Cys residues; furthermore, individual replacements of Cys2, -4, or -5 abolish DNA binding. In contrast, most replacements of Cys3 have little or no direct effect, but the observed binding is now resistant to alkylation or oxidation by diamide. In the absence of direct evidence for either a Cys3-SOH derivative or a disulfide involving Cys3 in the oxidized protein, however, it has not been possible to distinguish further between these two structures.

OxyR. Ironically, although OxyR was one of the first proteins for which a functional Cys-SOH redox center was proposed (*61*), as the basis for its ability to sense H_2O_2, the elegant work of Zheng et al. (*62*) has recently shown that a redox-active protein disulfide is present. Both Cys199 and Cys208 are essential for transcriptional activation by OxyR in vivo, and mass spectrometric analyses of tryptic digests with oxidized versus reduced forms of the OxyR4C → A mutant retaining only these two Cys residues confirmed the presence of the intramolecular disulfide, in agreement with the results of spectrophotometric disulfide assays. Formation of the Cys199−Cys208 disulfide in vivo leads to a conformational change within the OxyR−DNA complex that activates transcription, and on the basis of the relative in vivo sensitivities to the respective Cys mutations, Cys199 has been proposed as the H_2O_2 reaction center. Formation of Cys199-SOH is followed by rapid condensation with Cys208-SH to give the disulfide; this mechanism is directly comparable to that for oxidation of the wild-type AhpC Prx (*50*), with Cys199-SH serving as the functional equivalent of Cys46-SH in reduced AhpC.

Two specific aspects of OxyR structure and function have been indicated to contribute to its sensitivity toward H_2O_2. It should be added that although diamide and Cys-SNO offer partial activation of OxyR in vivo and in vitro, the protein appears to have evolved specifically to detect H_2O_2 and other peroxides (*62*). One factor that promotes the H_2O_2 sensitivity arises from the reported cooperativity for the H_2O_2 activation of tetrameric OxyR. A second factor relates to the active-site environment of Cys199-SH and its activation for nucleophilic attack on H_2O_2; sequence comparisons reveal that His198 and Arg201 flanking Cys199 in the *E. coli* protein are absolutely conserved in other OxyR homologues. This basic segment, which compares favorably with those

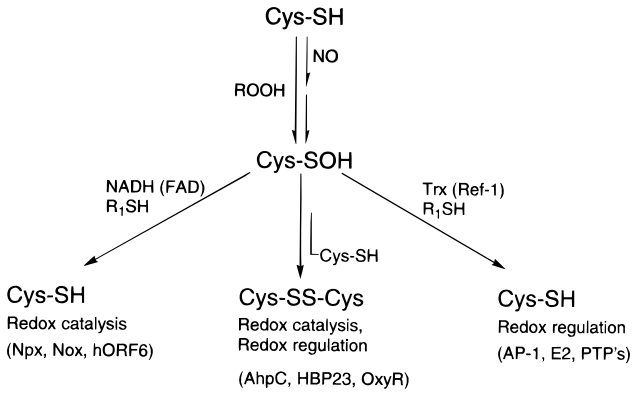

FIGURE 2: Diverse roles for protein-SOH in redox catalysis and redox regulation. R is H, FADH, or alkyl, and R_1SH is either GSH, DTT, or another as-yet-unidentified thiol(s).

found around the suspected Cys-SOH centers in Fos, Jun, and the E2 protein, may stabilize Cys199-S^- and otherwise contribute to a lowered activation energy for the reaction with H_2O_2. In fact, the second-order rate constant for the reaction of H_2O_2 with the OxyR4C → A mutant has been estimated (*63*) to be 2.3×10^5 M^{-1} s^{-1} (pH 7.0), which approaches the value of 3.0×10^6 M^{-1} s^{-1} determined for the EH_2 form of Npx at pH 7.0 and 5 °C (*64*). Under anaerobic conditions in vitro, in the presence of glutaredoxin 1 and GSH/GSSG ($E_h = -263$ mV), 2 μM H_2O_2 was still sufficient to transiently oxidize 1 μM OxyR completely within 30 s; the rapid reactions of reduced OxyR with even low concentrations of H_2O_2, both in vitro and in vivo, are much faster than glutaredoxin 1-mediated reduction, thus allowing for the desirable outcome of transient activation in a reducing environment.

SUMMARY

In addition to providing a structural and mechanistic foundation which should be useful in the evaluation of proposals involving Cys-SOH in redox catalysis and redox regulation (Figure 2), the reactivity data for Cys-SOH intermediates in the AhpC and HBP23 Prx proteins, OxyR, and even the Npx L40C mutant clearly demonstrate that Cys-SOH rapidly reacts with proximal Cys-SH to give the stable protein disulfide. In the context of oxidative Cys-SH modifications and nitrosative stress (*2*) therefore, it seems clear that SOH > SSR in order of reactivity; accordingly, we may expect the more reactive Cys-SOH to play an increasingly significant role in redox regulation, especially as the structural and chemical approaches surveyed in this report are applied to more of these systems. And, although the molecular basis of redox sensitivity in proteins is far from being completely understood, it appears that protein-SOH stabilization and function has become a very well-defined and established concept since Allison's original review in 1976. Current efforts in this and other laboratories are designed to bring about a greater understanding of Cys-SOH function in both redox and nonredox modes of enzyme catalysis.

ACKNOWLEDGMENT

We thank Dr. Masafumi Odaka and Dr. John Denu for their very helpful correspondence during the preparation of the manuscript, and we thank Prof. Toshio Hakoshima and Prof. Takeshi Nishino for providing a copy of their manuscript prior to publication. J.I.Y. also acknowledges the scientific support of Dr. Wim G. J. Hol (Department of Biological Structure, University of Washington, Seattle, WA).

REFERENCES

1. Nakamura, H., Nakamura, K., and Yodoi, J. (1997) *Annu. Rev. Immunol. 15*, 351−369.
2. Stamler, J. S., and Hausladen, A. (1998) *Nat. Struct. Biol. 5*, 247−249.
3. Allison, W. S. (1976) *Acc. Chem. Res. 9*, 293−299.
4. Kice, J. L. (1980) *Adv. Phys. Org. Chem. 17*, 65−181.
5. Hogg, D. R. (1990) in *The Chemistry of Sulphenic Acids and their Derivatives* (Patai, S., Ed.) pp 361−402, John Wiley & Sons, New York.
6. Claiborne, A., Miller, H., Parsonage, D., and Ross, R. P. (1993) *FASEB J. 7*, 1483−1490.
7. Goto, K., Holler, M., and Okazaki, R. (1997) *J. Am. Chem. Soc. 119*, 1460−1461.
8. Ishii, A., Komiya, K., and Nakayama, J. (1996) *J. Am. Chem. Soc. 118*, 12836−12837.
9. Tripolt, R., Belaj, F., and Nachbaur, E. (1993) *Z. Naturforsch. 48b*, 1212−1222.
10. Heckel, A., and Pfleiderer, W. (1983) *Tetrahedron Lett. 24*, 5047−5050.
11. Pal, B. C., Uziel, M., Doherty, D. G., and Cohn, W. E. (1969) *J. Am. Chem. Soc. 91*, 3634−3638.
12. Liu, T.-Y. (1977) in *The Proteins* (Neurath, H., and Hill, R. L., Eds.) 3rd ed., Vol. 3, pp 239−402, Academic Press, New York.
13. Yeh, J. I., Claiborne, A., and Hol, W. G. J. (1996) *Biochemistry 35*, 9951−9957.
14. Williams, C. H., Jr. (1992) in *Chemistry and Biochemistry of Flavoenzymes* (Müller, F., Ed.) Vol. III, pp 121−211, CRC Press, Boca Raton, FL.
15. Stehle, T., Ahmed, S. A., Claiborne, A., and Schulz, G. E. (1991) *J. Mol. Biol. 221*, 1325−1344.
16. Claiborne, A., Ross, R. P., and Parsonage, D. (1992) *Trends Biochem. Sci. 17*, 183−186.
17. Parsonage, D., and Claiborne, A. (1995) *Biochemistry 34*, 435−441.
18. Mallett, T. C., and Claiborne, A. (1998) *Biochemistry 37*, 8790−8802.
19. Crane, E. J., III, Vervoort, J., and Claiborne, A. (1997) *Biochemistry 36*, 8611−8618.
20. Mande, S. S., Parsonage, D., Claiborne, A., and Hol, W. G. J. (1995) *Biochemistry 34*, 6985−6992.
21. Poole, L. B., and Claiborne, A. (1989) *J. Biol. Chem. 264*, 12330−12338.
22. Crane, E. J., III, Parsonage, D., and Claiborne, A. (1996) *Biochemistry 35*, 2380−2387.
23. Karplus, P. A., and Schulz, G. E. (1989) *J. Mol. Biol. 210*, 163−180.
24. Veeraraghavan, S., Mello, C. C., Lee, K. M., Androphy, E. J., and Baleja, J. D. (1998*) J. Biomol. NMR 11*, 457−458.
25. McBride, A. A., Klausner, R. D., and Howley, P. M. (1992) *Proc. Natl. Acad. Sci. U.S.A. 89*, 7531−7535.
26. Mallett, T. C., Parsonage, D., and Claiborne, A. (1999) *Biochemistry 38*, 3000−3011.
27. Ahmed, S. A., and Claiborne, A. (1989) *J. Biol. Chem. 264*, 19864−19870.
28. Miller, H., Mande, S. S., Parsonage, D., Sarfaty, S. H., Hol., W. G. J., and Claiborne, A. (1995) *Biochemistry 34*, 5180−5190.
29. Becker, K., Savvides, S. N., Keese, M., Schirmer, R. H., and Karplus, P. A. (1998*) Nat. Struct. Biol. 5*, 267−271.
30. Becker, K., Gui, M., and Schirmer, R. H. (1995) *Eur. J. Biochem. 234*, 472−478.
31. Hausladen, A., Privalle, C. T., Keng, T., DeAngelo, J., and Stamler, J. S. (1996) *Cell 86*, 719−729.

32. Keese, M. A., Böse, M., Mülsch, A., Schirmer, R. H., and Becker, K. (1997) *Biochem. Pharmacol. 54*, 1307−1313.
33. Butzer, U., Weidenbach, H., Gansauge, S., Gansauge, F., Beger, H. G., and Nussler, A. K. (1999) *FEBS Lett. 445*, 274−278.
34. Nagashima, S., Nakasako, M., Dohmae, N., Tsujimura, M., Takio, K., Odaka, M., Yohda, M., Kamiya, N., and Endo, I. (1998) *Nat. Struct. Biol. 5*, 347−351.
35. Kobayashi, M., and Shimizu, S. (1998) *Nat. Biotechnol. 16*, 733−736.
36. Odaka, M., Fujii, K., Hoshino, M., Noguchi, T., Tsujimura, M., Nagashima, S., Yohda, M., Nagamune, T., Inoue, Y., and Endo, I. (1997) *J. Am. Chem. Soc. 119*, 3785−3791.
37. Nakasako, M., Odaka, M., Yohda, M., Dohmae, N., Takio, K., Kamiya, N., and Endo, I. (1999) *Biochemistry 38*, 9887−9898.
38. Tsujimura, M., Dohmae, N., Odaka, M., Chijimatsu, M., Takio, K., Yohda, M., Hoshino, M., Nagashima, S., and Endo, I. (1997) *J. Biol. Chem. 272*, 29454−29459.
39. Nojiri, M., Yohda, M., Odaka, M., Matsushita, Y., Tsujimura, M., Yoshida, T., Dohmae, N., Takio, K., and Endo, I. (1999) *J. Biochem. 125*, 696−704.
40. Katayama, Y., Matsushita, Y., Kaneko, M., Kondo, M., Mizuno, T., and Nyunoya, H. (1998) *J. Bacteriol. 180*, 2583−2589.
41. DeMaster, E. G., Quast, B. J., Redfern, B., and Nagasawa, H. T. (1995) *Biochemistry 34*, 11494−11499.
42. Denu, J. M., and Dixon, J. E. (1998) *Curr. Opin. Chem. Biol. 2*, 633−641.
43. Chae, H. Z., Robison, K., Poole, L. B., Church, G., Storz, G., and Rhee, S. G. (1994) *Proc. Natl. Acad. Sci. U.S.A. 91*, 7017−7021.
44. Schröder, E., and Ponting, C. P. (1998) *Protein Sci. 7*, 2465−2468.
45. Choi, H.-J., Kang, S. W., Yang, C.-H., Rhee, S. G., and Ryu, S.-E. (1998) *Nat. Struct. Biol. 5*, 400−406.
46. Hirotsu, S., Abe, Y., Okada, K., Nagahara, N., Hori, H., Nishino, T., and Hakoshima, T. (1999) *Proc. Natl. Acad. Sci. U.S.A. 96* (in press).
47. Kang, S. W., Baines, I. C., and Rhee, S. G. (1998) *J. Biol. Chem. 273*, 6303−6311.
48. Chae, H. Z., Chung, S. J., and Rhee, S. G. (1994) *J. Biol. Chem. 269*, 27670−27678.
49. Poole, L. B. (1996) *Biochemistry 35*, 65−75.
50. Ellis, H. R., and Poole, L. B. (1997) *Biochemistry 36*, 13349−13356.
51. Ellis, H. R., and Poole, L. B. (1997) *Biochemistry 36*, 15013−15018.
52. Lundblad, R. L., and Noyes, C. M. (1984) *Chemical Reagents for Protein Modification*, Vol. I, CRC Press, Boca Raton, FL.
53. Denu, J. M., and Tanner, K. G. (1998) *Biochemistry 37*, 5633−5642.
54. Lee, S.-R., Kwon, K.-S., Kim, S.-R., and Rhee, S. G. (1998) *J. Biol. Chem. 273*, 15366−15372.
55. Xanthoudakis, S., and Curran, T. (1996) *Adv. Exp. Med. Biol. 387*, 69−75.
56. Xanthoudakis, S., Miao, G. G., and Curran, T. (1994) *Proc. Natl. Acad. Sci. U.S.A. 91*, 23−27.
57. Gorman, M. A., Morera, S., Rothwell, D. G., de La Fortelle, E., Mol, C. D., Tainer, J. A., Hickson, I. D., and Freemont, P. S. (1997) *EMBO J. 16*, 6548−6558.
58. Rothwell, D. G., Barzilay, G., Gorman, M., Morera, S., Freemont, P., and Hickson, I. D. (1997) *Oncol. Res. 9*, 275−280.
59. Hegde, R. S., Grossman, S. R., Laimins, L. A., and Sigler, P. B. (1992) *Nature 359*, 505−512.
60. Bandyopadhyay, S., and Gronostajski, R. M. (1994) *J. Biol. Chem. 269*, 29949−29955.
61. Storz, G., Tartaglia, L. A., and Ames, B. N. (1990) *Science 248*, 189−194.
62. Zheng, M., Åslund, F., and Storz, G. (1998) *Science 279*, 1718−1721.
63. Åslund, F., Zheng, M., Beckwith, J., and Storz, G. (1999) *Proc. Natl. Acad. Sci. U.S.A. 96*, 6161−6165.
64. Crane, E. J., III, Parsonage, D., Poole, L. B., and Claiborne, A. (1995) *Biochemistry 34*, 14114−14124.

BI992025K